

Visualization of the Effect of Additional Fertilization on Paddy Rice by Time-Series Analysis of Vegetation Indices using UAV and Minimizing the Number of Monitoring Days for its Workload Reduction

Taichi Ito^{1,*}, Ken'ichi Minamino¹, Shintaro Umeki²

¹Graduate School of Software and Information Science, Iwate Prefectural University, Takizawa, 0200611, Japan

²Hanamaki Satellite, Research Center for Industrial Science and Technology, Iwate University, Hanamaki, 0250312, Japan

ARTICLE INFO

Article history:

Received: 14 March, 2024

Revised: 2 May, 2024

Accepted: 4 May, 2024

Online: 25 May, 2024

Keywords:

Additional Fertilization

Machine Learning

Paddy Rice

Time-Series Clustering

Unmanned Aerial Vehicle

Vegetation Index

ABSTRACT

This research is an extension of the research (ISEEIE 2023), which dealt with Time-Series Clustering (TSC) of Vegetation Index (VI) for paddy rice. The novelty of this research is "Visualization of growth changes before and after additional fertilization," "Analyzing the appropriate amount of additional fertilizer," and "Optimization of monitoring period to minimize the number of monitoring days for its workload reduction using Unmanned Aerial Vehicle (UAV)." For visualization of growth changes before and after fertilization, a UAV was used to obtain VIs for each mesh and make its time-series data during the monitoring period. Then, TSC was performed on the data. As a result of clustering, NDVI and NDRE increased with additional fertilizer, making it possible to visualize the fertilizer effects. For analyzing the appropriate amount of fertilizer, the its amount applied was changed for each paddy field (2.8, 3.5, 4.2g/m²). In a field experiment conducted, both the TSC results and the crop estimates by unit acreage sampling for each paddy field revealed no difference in yield among fields, indicating that the paddy field with the least fertilizer amount (2.8g/m²) is optimal. It was estimated that this would reduce nitrate nitrogen, which is harmful to soil and the human body, by 0.070mg/L. In addition, for optimization of the monitoring period, the importance of each independent variable outputted by Random Forest (RF) was used to find a subset of monitoring dates. In any VI, there is a period, determined by the range of effective accumulated temperature, when the clustering result does not change even if the number of monitoring dates is reduced (The period could be reduced from 30 to 40 days, which is particularly important for three vegetation indices). From these results, the technologies can help reduce fertilizer costs, excessive fertilization and environmental impacts, and promote the use of UAV.

1. Introduction

This paper is an extension of work originally presented at the 3rd International Symposium on Electrical, Electronics, and Information Engineering (ISEEIE 2023) [1].

A long-standing problem in Japanese agriculture is the aging and decline of farmers. According to a survey, from 2015 to 2020, the number of farmers decreased by approximately 22% to 1,363,000, and the percentage of those aged 65 years or older increased by 5% to 69.6% [2]. The main causes of this are that

appropriate farm work requires tacit knowledge and much human labor. Regarding the former, appropriate work is based on the heuristics of experts; therefore, it is difficult to share. Regarding the latter, Japan's agricultural fields are small, and mechanization has not yet progressed. These problems create barriers for new farmers and lead older farmers to quit farming. To solve this problem, "Smart Agriculture" is being promoted. Specifically, production management systems and the automatic operation of agricultural machinery are expected to clarify and save labor in farm work. However, these technologies are expensive and difficult to implement by farmers. Therefore, in this study, crop monitoring using unmanned aerial vehicles (UAV) was adopted, which is more reasonable than other technologies.

Corresponding Author: Taichi Ito, Iwate Prefectural University, Takizawa, 0200611, Japan, s236w001@s.iwate-pu.ac.jp

In UAV monitoring, multispectral cameras are often used to obtain the sunlight reflectance of crop leaves in various bands. Generally, healthy crops have high reflectance in the near-infrared band and low reflectance in the red band. However, in stressed crops, the difference in reflectance between the two bands decreases, as shown in Figure 1 [3], [4]. Based on this reflection characteristic, many vegetation indices (VI) have been developed using calculation formulas to understand vegetation conditions [5]. For example, using VIs, studies have created rice yield maps using the Normalized Difference Vegetation Index (NDVI) and the Normalized Difference Red Edge Index (NDRE) [6], [7]. These studies have shown that the VI value in the young panicle formation stage and the heading stage are correlated with yield; therefore, yield prediction is possible. However, these predictive models cannot be applied everywhere but within the research environment. Furthermore, despite multiple monitoring sessions, the model predicted using only the VI value input during the heading stage. In Japan, yield is important for planning rice demand and supply. Therefore, early and highly accurate predictions with numerous features are required.

This study focused on additional fertilization during farming. This study is important because it directly influences growth and yield. Generally, this work is conducted between the young panicle-forming and heading stages to supply nitrogen and potassium and can be expected to increase yield by enriching the contents of ears [8]. However, excessive fertilizer causes lodging owing to overgrowth, releasing water from the roots due to osmotic pressure, and health hazards owing to nitrate-nitrogen dissolution into groundwater [9], [10]. For nitrate-nitrogen, the Japanese standard value for water pollution is set at 10 mg/L [11]. Based on

these negative effects, it is necessary to determine the appropriate amount of fertilizer and apply variable fertilization. Because the effect of farm work appears gradually, it is important to compare it before and after work. Therefore, in this study, we use a new method of time-series analysis of VIs obtained from a UAV to visualize the vegetation before and after additional fertilization and analyze the appropriate fertilization amount. Furthermore, to reduce the workload of UAV monitoring, we use random forest (RF) to minimize the monitoring period.

2. Method

2.1. Monitoring

The monitoring targeted paddy fields owned by private farmers in Hanamaki City in Iwate Prefecture, Japan, and yielded 10 analysis results for six sites from 2021 to 2023 [1] [12] [13]. Several sites were used in the experiment, and the additional fertilizer amount varied for each field. This is because growth differences were observed for each fertilizer amount.

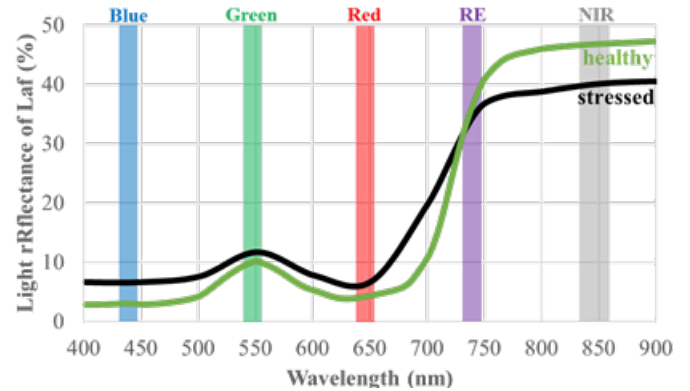


Figure 1: Spectral reflection characteristics of plants [1] [12] [13]

Table 1: Site and Cropping Information

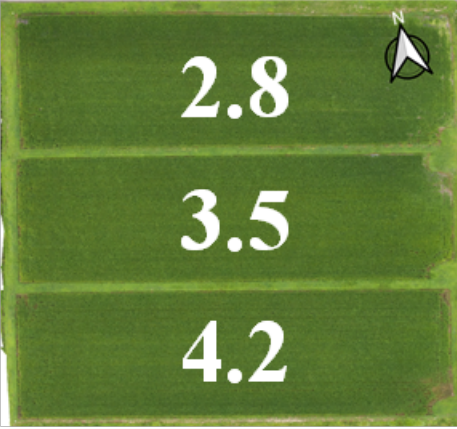
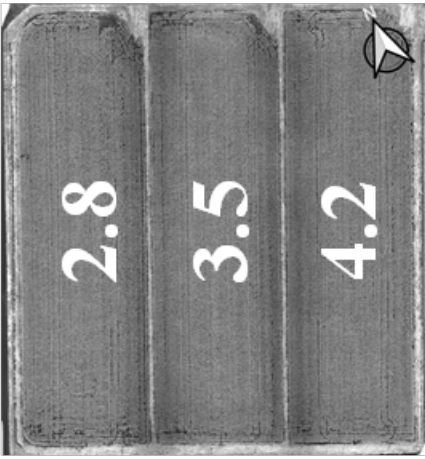
		Yuguchi-8 (2022)	Yuguchi (2023)
Variety		Yumi-azusa	Homusume-mai
Date	Number of Meshes	819	857
	Transplanting	May 7	May 5
	Additional Fertilization	Jul. 20	Middle Jul.
	Heading	Aug. 3	Late Jul.
	Harvest	Oct. 6	Late Sep.
Aerial photo. & Fertilizer Amount [gN/m^2]			



Figure 2: UAV used for monitoring (Phantom 4 Multispectral)

Table 1 shows the sites and cropping information where the comparative fertilizer application experiments were conducted (Yuguchi-8 in 2022 and Yuguchi in 2023). The distance between the two fields was approximately 1 km; therefore, the weather conditions were similar. Both fields are adjacent to each other and can be divided into North, Center, and South in Yuguchi-8, and West, Center, and East in Yuguchi. Fertilizer amounting to 2.8, 3.5, and 4.2 gN/m² was applied in the middle of July using a pesticide spraying UAV (AGRAS MG-1, DJI Co., Ltd. [14]).

To calculate the VI, a UAV equipped with a multispectral camera is required. Thus, a UAV (Phantom 4 Multispectral, DJI Co., Ltd.), shown in Figure 2 was used. It weighs 1,487 g, has a maximum flight time of 27 min, and has a multispectral camera with one RGB sensor for visible light and five monochrome sensors for multispectral light. The bands of the monochrome sensor were 450 nm (blue), 560 nm (green), 650 nm (red), 730 nm (red edge: RE), and 840 nm (near-infrared: NIR) [15]. The flight altitude was set to 30 m, and orthogonal images of each band were created after monitoring. The VI values were then calculated from these orthoimages. The VIs calculated in this study were (1), (2), and (3).

$$NDVI = (R_{NIR} - R_{Red}) / (R_{NIR} + R_{Red}) \quad (1)$$

$$NDRE = (R_{NIR} - R_{RE}) / (R_{NIR} + R_{RE}) \quad (2)$$

$$sNDRE = (NDRE - \mu_{NDRE}^d) / \sigma_{NDRE}^d \quad (3)$$

where

R_b : Reflectance of band "b"

μ_{NDRE}^d : Average of NDRE on date "d"

σ_{NDRE}^d : Standard Deviation of NDRE on date "d"

The NDVI was used for vegetation diagnosis. This was calculated by normalizing the NIR and Red bands. It is widely used; however, it has been reported that the soil easily affects it, and the index becomes saturated during the peak vegetation season [6], [16], [17]. The NDRE was used to diagnose crop stress and nitrogen content. The RE band reaches deeper into the canopy than the Red band; therefore, stress can be detected earlier. Additionally, it is not easily saturated; therefore, depending on the season, it may be more appropriate than NDVI for diagnosing vegetation and yield [7], [17], [18]. A Standardized Normalized Difference Red Edge Index (sNDRE) was developed to ensure that the NDRE did not change unless it was under significant stress. This is the relative value for each date and is used for a relative comparison within a field [1], [12], [13]. In addition, it uses only NDRE for calculations,

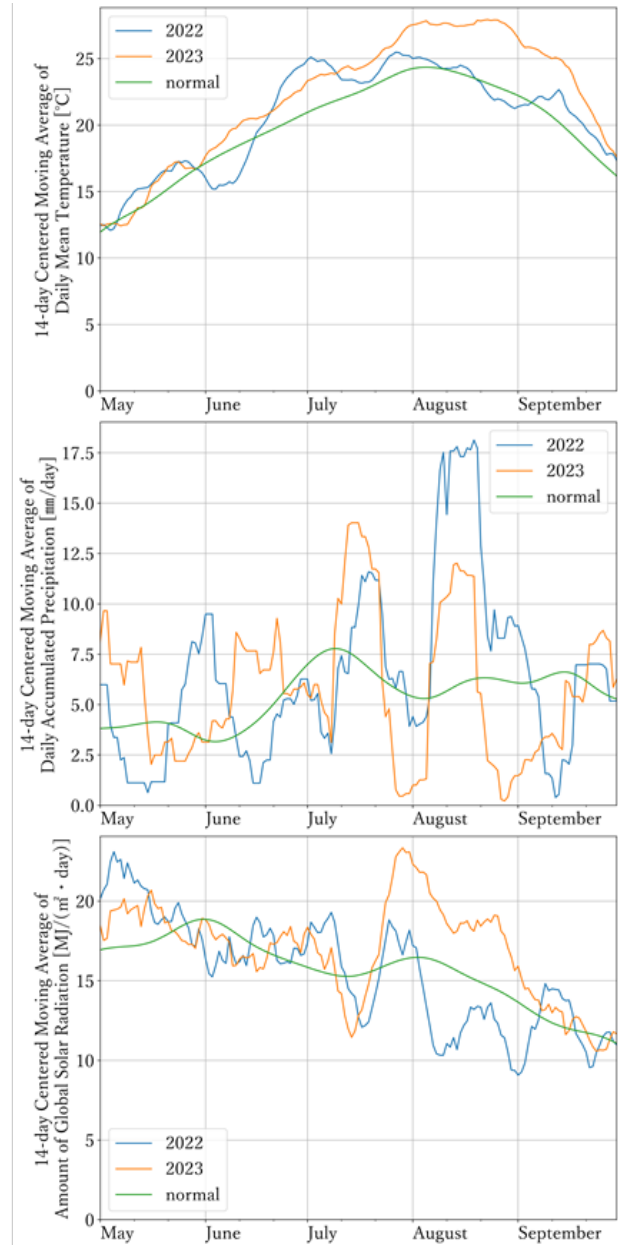


Figure 3: Meteorological data at the experimental field (Daily mean temperature, Precipitation, and Solar radiation)

and it is possible to diagnose the relative stress and nitrogen content levels in the field.

After computing these three VIs, meshes were created in the rice field portion of the orthoimage. The mesh size was 3 m square.

The VI of each mesh was determined as the average VI value of pixels within the mesh. After computing the VIs of all meshes on all monitoring dates, VI time-series data were generated for each mesh.

Figure 3 shows the 14-day centered moving average of the daily mean temperature, accumulated precipitation, and global solar radiation at Yuguchi during the rice-growing period (May to September) in 2022, 2023, and a normal year. As a characteristic point, there was heavy rainfall in August 2022 and high

temperatures in 2023. To adjust for these weather differences, monitoring dates were converted to growth stages using the Effective Accumulated Temperature (EAT) from the transplantation date and paddy rice growth model [19], [20]. Table 2 shows the correspondence between the EAT and growth stages, and Figure 4 shows the relationship between the growth stages and dates for both years.

2.2. Evaluation of Additional Fertilization

To visualize the fertilization effect, this research used time-series clustering (TSC) with the K-Means++ method on the VI time-series data presented in Section 2.1. Clustering usually classifies 2 or 3-dimensional data which can be shown in scatter diagrams [21]. However, this analysis aimed to classify time-series data. Therefore, a program was developed to handle time-series

data with several missing monitoring dates [1]. This program is an improved version of the function “TimeSeriesKMeans” [22] in the Python library “tslearn.” This program was used in this research to conduct TSC. The elbow method [1], [23] was used to determine the number of clusters. From the TSC results, the VI time-series transition of each cluster's centroid, cluster distribution, and cluster ratio for each paddy field were obtained. Based on these results, we determined the growth differences according to the fertilizer amount and the appropriate fertilizer amount. Furthermore, a crop estimate by unit acreage sampling was conducted immediately before harvest to confirm the consistency between the appropriate fertilizer amount determined by TSC analysis and the actual yield. The sampling method was to select five meshes per field so that the heading-stage NDVI was scattered, and five stubbles per mesh were collected. The selected meshes are listed in Table 3.

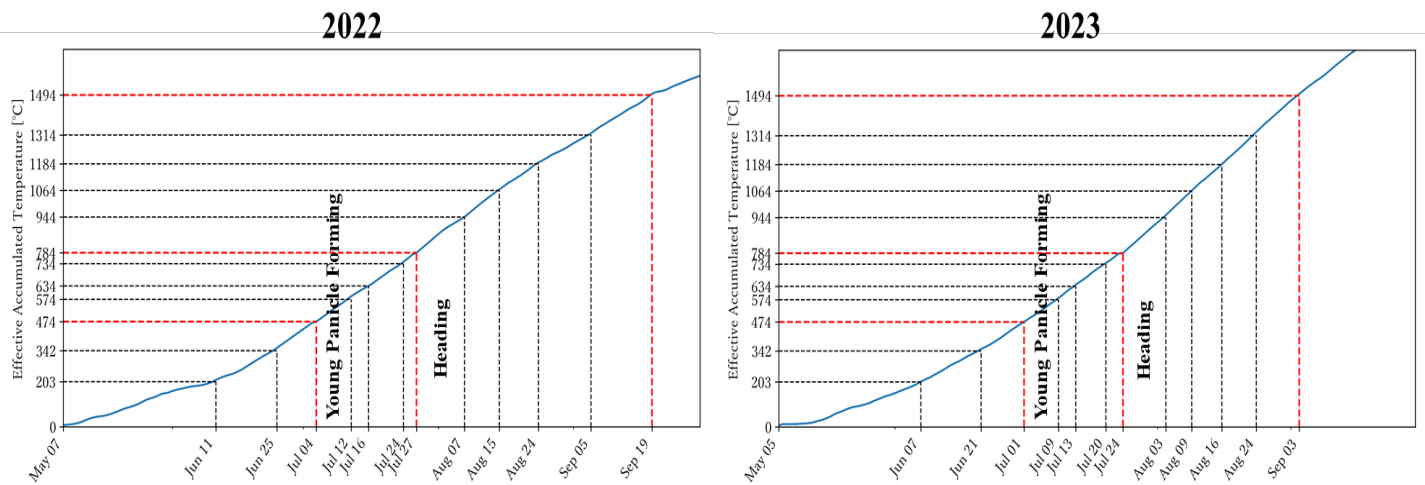


Figure 4: Relationship between the growth stages and dates in 2022 and 2023

Table 2: Correspondence between growth stage and EAT

Model	Effective & Upper limit temperature	Growth Stage	Required EAT [°C]
Leaf number on the main culm	Effective: 10°C Upper limit: 24°C	Slow leaf emergence	0
		Turning leaf emergence rate	203
		Fast leaf emergence	342
Young panicle development	Effective: 10°C	Young panicle forming	474
		Pollen mother cell differentiation	574
		Meiosis	634
		Pollen accumulation	734
		Heading	784
Brown Rice Development	Effective: 10°C	Milk Ripe	944
		Dough Ripe	1064
		Yellow Ripe	1184
		Full Ripe	1314
		Harvest	1494

2.3. Optimization of Monitoring Period

Previous studies have analyzed healthy vegetation growth, stress, etc. in paddy rice using the TSC of VI time-series data [12], [13]. However, UAV monitoring, such as moving to sites, preparing for flight, and computing VI values from aerial photographs, takes time. Therefore, a survey was conducted to identify the subset of monitoring dates for which the feature quantity was not reduced significantly [1]. RF was used in this survey. This was adopted because it can handle the categorical values that are the output results of TSC (i.e., cluster ID) and it outputs the importance of each independent variable (monitoring date). The execution conditions for RF are listed in Table 4 [1]. From the RF, a classifier model was created that outputs the cluster ID when given the VI time-series data of each mesh. The optimization method is shown in Figure 5. First, a classifier was created using the training data of the VI time series over the entire period (Entire RF). Second, the optimized period was determined based on the importance of the test data given to the classifier. Third, another classifier was created using the training data of the VI time series values in the optimized period (Optimized RF). Fourth, the cluster ID match percentages were calculated when classifying the test data between the TSC and Entire RF ($pppp_{RRReee}$) and between the TSC and Optimized RF ($pppp_{ooooee}$). Finally, the McNemar's test was performed with the null hypothesis as " $pp_{RRReee} = ppp_{ooooee}$ "

and it was evaluated that optimization was successful if the null hypothesis was not rejected. Using this method, the optimized period was determined from the monitoring data of eight sites (excluding the two sites in Table 1 from the monitoring data of all ten sites). This confirmed the consistency between the appropriate fertilizer amount using TSC analysis results in the optimized period and the actual yield.

3. Results

3.1. Comparison of Additional Fertilizer Amounts

Table 5 presents the yields of the five sampled meshes at both sites. Sample 5 from West of Yuguchi was missing because the survey was discontinued. The sampled yield was calculated as the weight of five stubbles. These units were converted to SI units, and the average for each rice field is shown in the second line from the bottom. The bottom line shows the p-value of the Kruskal-Wallis test (non-parametric, unpaired, differences between three or more groups) with the null hypothesis set as "the average of sampled yields of all rice fields are equal." As a result, the null hypothesis was adopted even at the 10% significance level, as the p-value for both sites significantly exceeded 0.1.

For the entire TSC period, the time-series transitions in each cluster centroid, cluster ID distribution map, and percentage of

Table 3: Sampled meshes

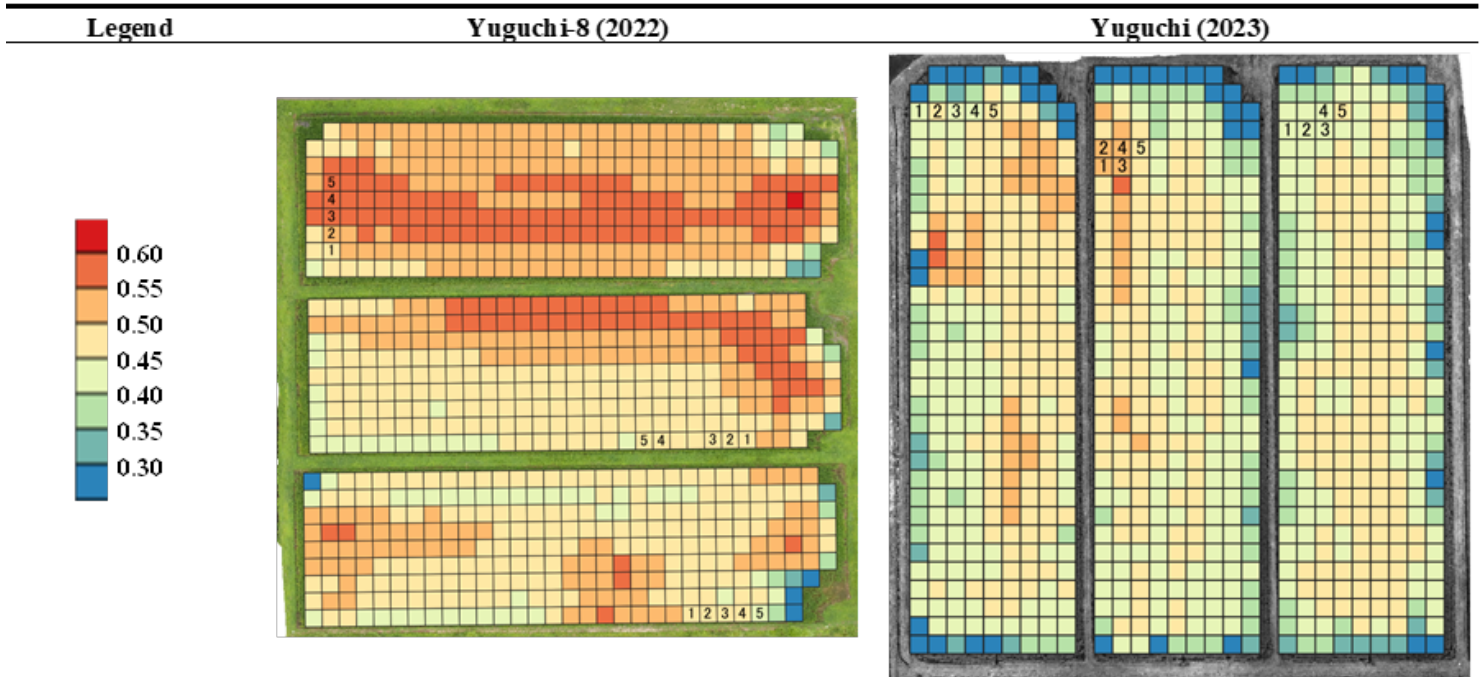


Table 4: Execution conditions of RF

Item	Condition
Independent Valuable	Time-series VI value per monitoring date of each mesh
Dependent Valuable	Cluster ID of each mesh
Training Data	Sampling by Stratified Sampling with Cluster ID as a layer (25% of total meshes)
Test Data	Remaining 75% of total meshes

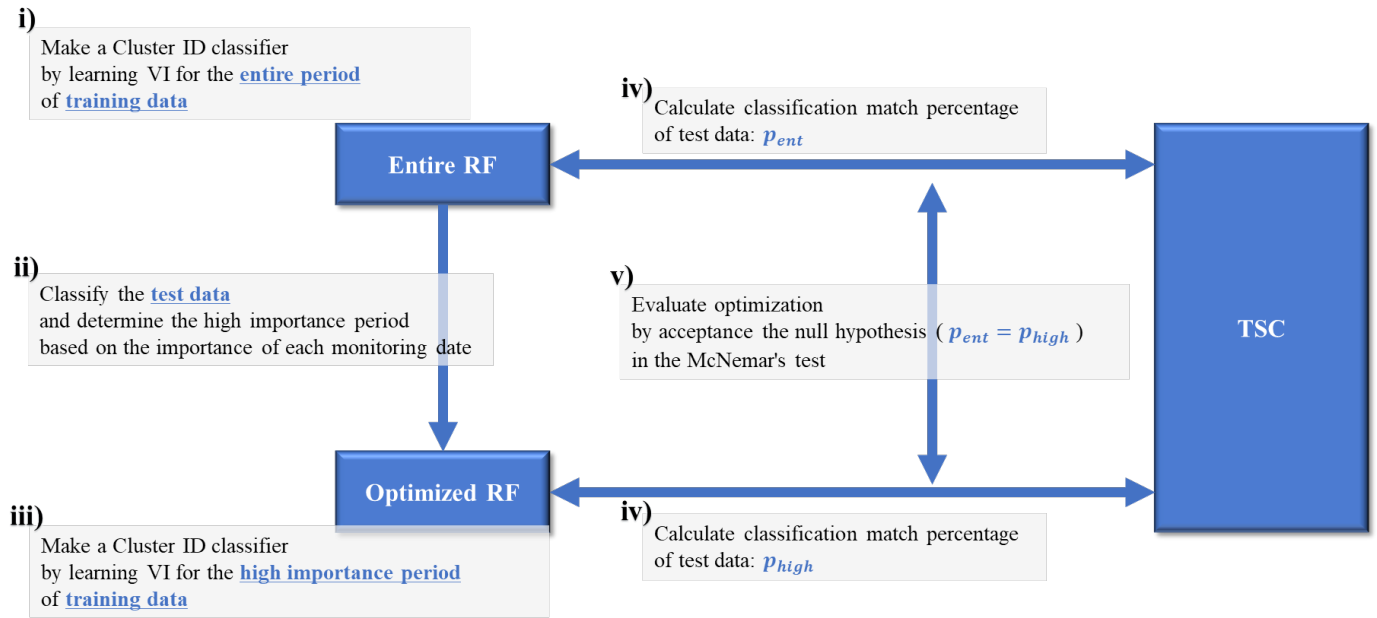


Figure 5: Method of monitoring period optimization

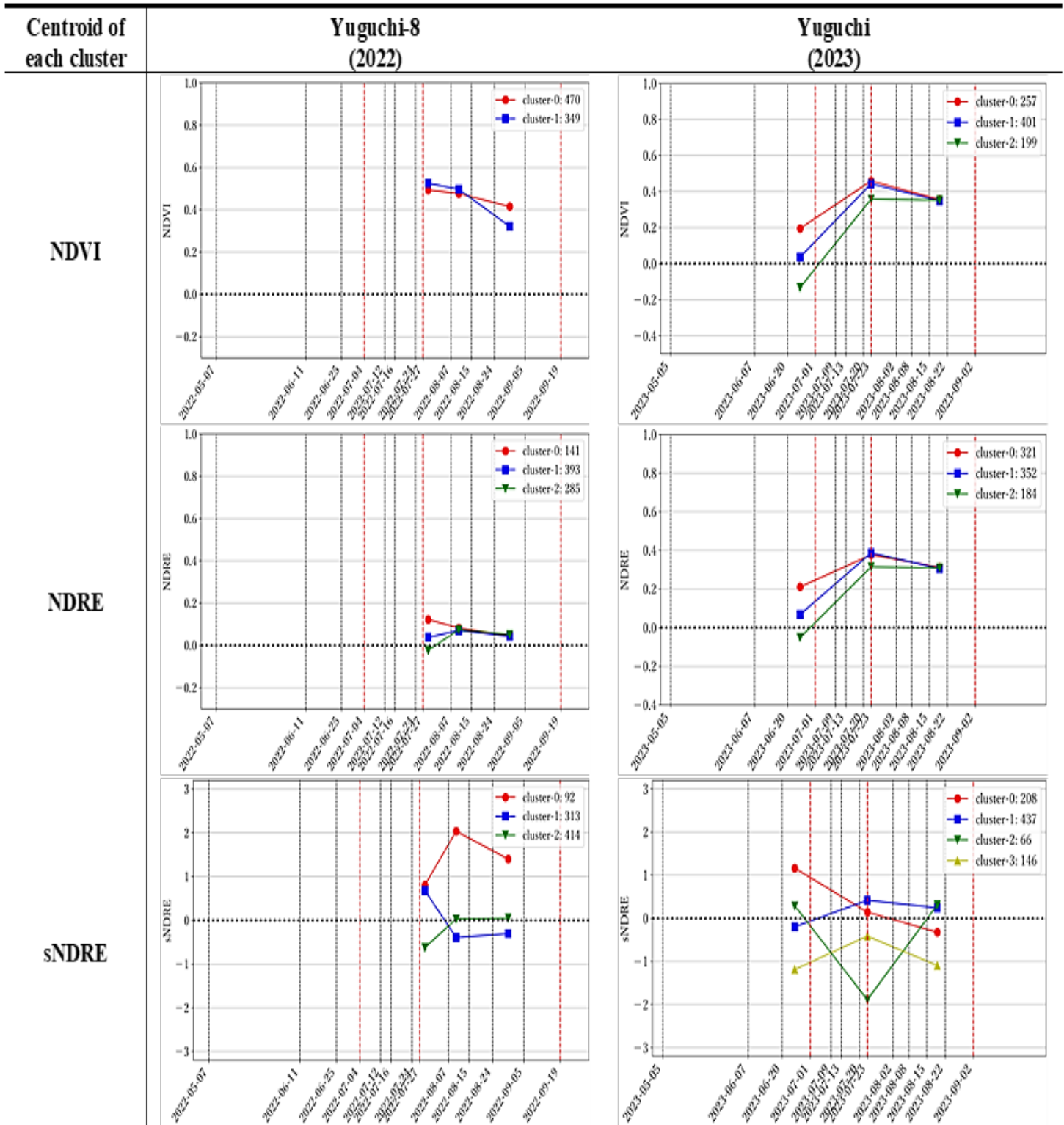
Table 5: Yields of 5 sampled meshes and results of Kruskal-Wallis test

g / 5stubbles	Yuguchi-8 (2022)			Yuguchi (2023)		
	North	Center	South	West	Center	East
Sample1	176.0	180.8	220.6	136.4	161.8	221.9
Sample2	239.0	172.2	188.4	203.0	66.6	175.7
Sample3	189.6	192.0	164.0	190.5	204.8	142.0
Sample4	180.2	178.2	155.6	177.6	214.3	206.9
Sample5	213.0	175.8	139.2	N/A	181.5	178.0
Average	199.6	179.8	173.6	176.9	165.8	184.9
Standard Deviation	26.3	7.5	31.7	28.9	59.1	30.9
Average [g/mm ²]	724	653	630	642	602	671
p-value of Kruskal-Wallis Test	0.249			0.873		

each cluster are shown in Table 6, Table 7, and Table 8. For Yuguchi-8 in 2022, the meshes were classified into two, three, and three clusters for NDVI, NDRE, and sNDRE, respectively. For the NDVI, there was no difference between clusters in the heading stage, and the yields were expected to be similar in all rice fields. In the NDRE, differences were observed at the heading stage, but no differences were observed thereafter. Cluster-0, which had relatively low stress, was found near the ridges. In sNDRE, Cluster-0 was high and often observed near the ridge. The central meshes of each paddy field were many Clusters-1 and Cluster-2, but after heading, the value did not differ by more than 0.5, with no difference in the stress level. The same can be said for all three rice fields, and no growth differences were observed between them. Therefore, the appropriate fertilizer amount was analyzed as the north field (2.8 gN/m²), where the amount is the lowest, considering fertilizer costs etc.

At Yuguchi in 2023, the meshes were classified into three, three, and four clusters for NDVI, NDRE, and sNDRE, respectively. In the NDVI, there was a difference of approximately 0.15 between clusters at the first monitoring. However, the low value (Cluster-2) improved because of the fertilizer. Thus, it was concluded that there was no difference in growth between the fields because the value of each cluster was similar at the heading stage. There was a large difference in sNDRE between the four clusters. Similar to other VI, high-value (Cluster-0 and Cluster-1) were observed at the center of the field. These two clusters appeared slightly more frequently in the West and Center. Similar

Table 6: Centroid of each cluster (entire period)



to Yuguchi-8, the same was observed for all three fields, but no growth differences were observed. Therefore, the appropriate amount of fertilizer was analyzed in the western field (2.8 gN/m²).

3.2. Optimization of Monitoring Period

The importance results for the six sites (excluding Yuguchi-

8 in 2022 and all sites in 2023) are shown in Figure 6. The vertical axis in this figure represents the Relative Importance. The Importance output by the RF is the percentage contribution [1], [24]. That is, the fewer the monitoring dates, the higher the value. To adjust for this, Relative Importance was calculated by dividing the usual output importance by the reciprocal of the number of monitoring dates [1]

Table 7: Cluster ID distribution map (entire period)

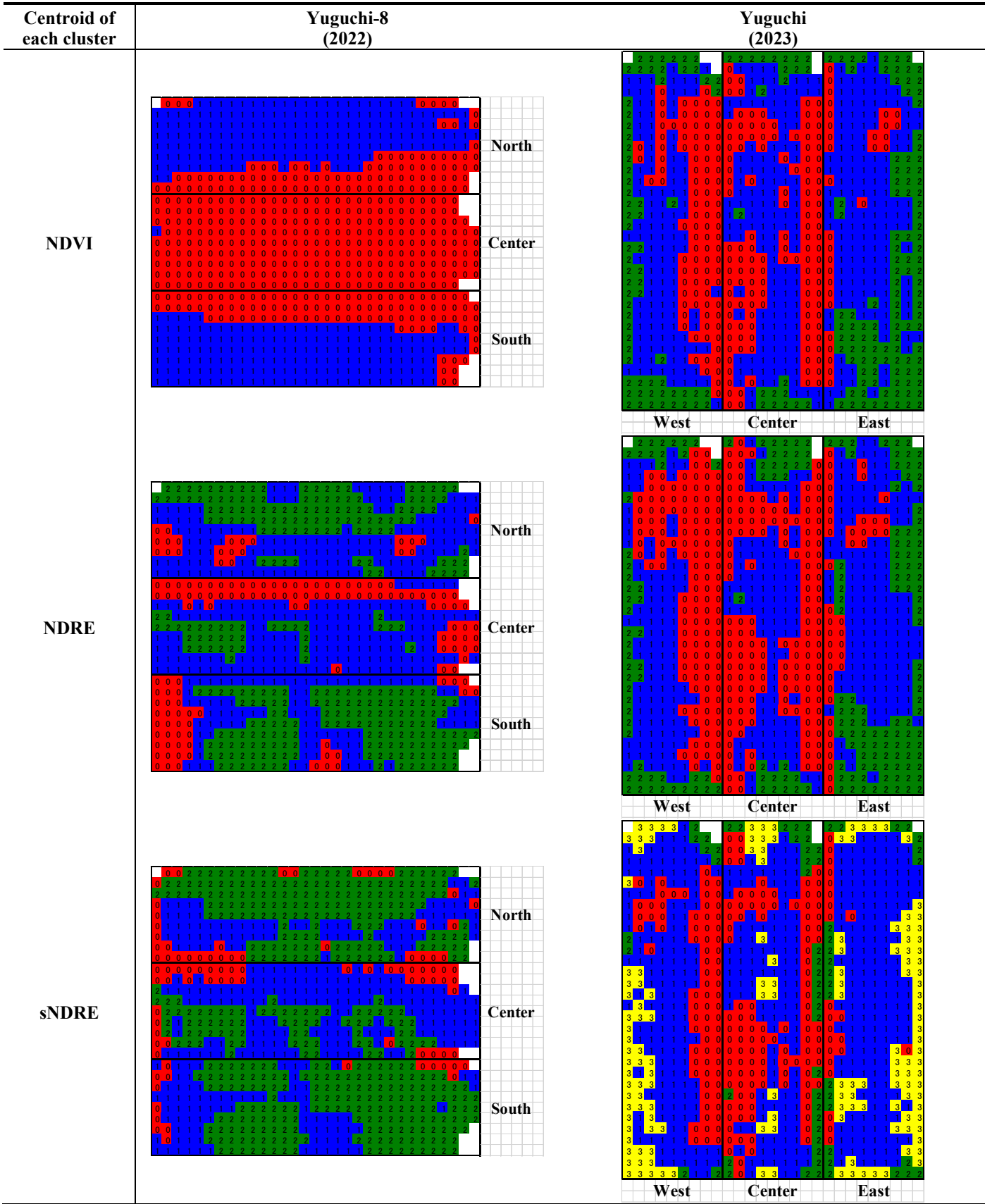
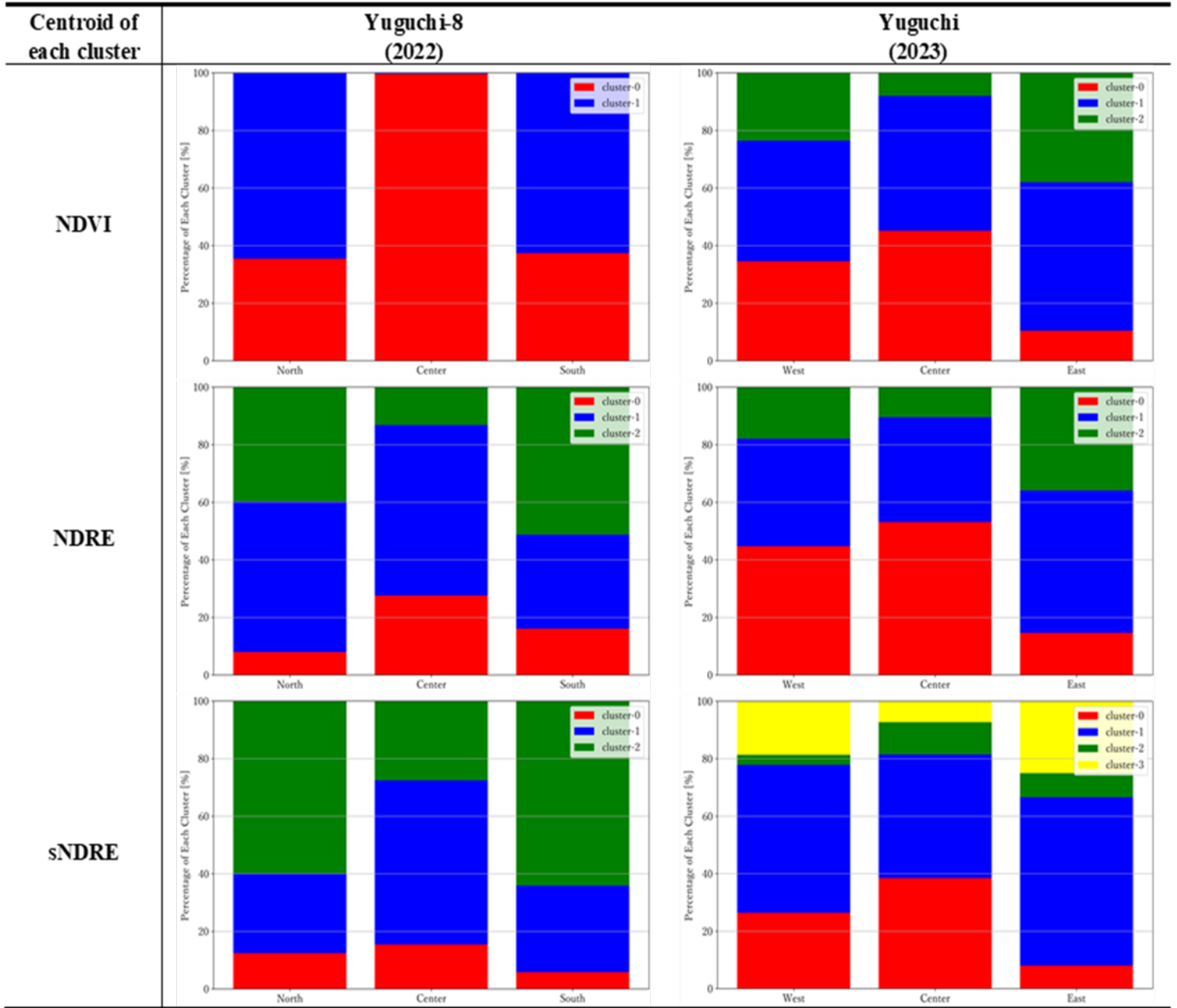


Table 8: Percentage of each cluster (entire period)



[24]. To optimize the optimization method of monitoring period, first, the initial period was extracted, for which the minimum period included all data with a Relative Importance of one or more. Next, the period was expanded or deduced to the

sum of the Relative Importance of 49% to 51%, in contrast to the entire period shown in Figure 6.

The optimized periods of the EAT determined using this method are listed in Table 9. The rightmost column shows the EATs of the optimized period converted to dates using the EAT from May 7 in a normal year. The optimal period for all VIs was approximately one month. This period was from the young panicle forming to the milk ripe for NDVI and NDRE, and from heading to the full ripe for sNDRE. In Table 10, the results are applied to two sites that were excluded when calculating the optimized period (i.e., Yuguchi -8 in 2023 and Yuguchi in 2022). For the match rate

of the cluster ID classification of the test data between the Entire RF and TSC (p_{ent}), and the Optimized RF and TSC (p_{opt}), p_{opt} was greater than p_{ent} . They are not necessarily 100% because the training data comprise 25% of all the meshes and the remaining 75% of the test data. The rightmost column shows the p-value of the test for the difference between two percentages. No VI was significant at the 5% level. In other words, the monitoring period can be optimized without significantly reducing the classification accuracy. In addition, although the 2023 data were not used to derive the optimized period, p_{opt} of Yuguchi had high accuracy (over 98%). This indicates that the optimized period can be derived using the EAT without depending on the year.

4. Discussion

4.1. Visualization of Paddy Rice Growth

In the TSC during the optimized period, most results showed that growth was different in the center of the fields and near the ridge. In the NDVI and NDRE, the area near the ridge was classified into low-value clusters, so it is thought that the vegetation growth and stress states were not better than those in the center of the field. In contrast, for the sNDRE at Yuguchi-8, the near-ridge meshes were classified into high-value clusters. It is thought that the amount of nitrogen was high because the fertilizer was washed away by heavy rain in August, (Figure 3, Table 7).

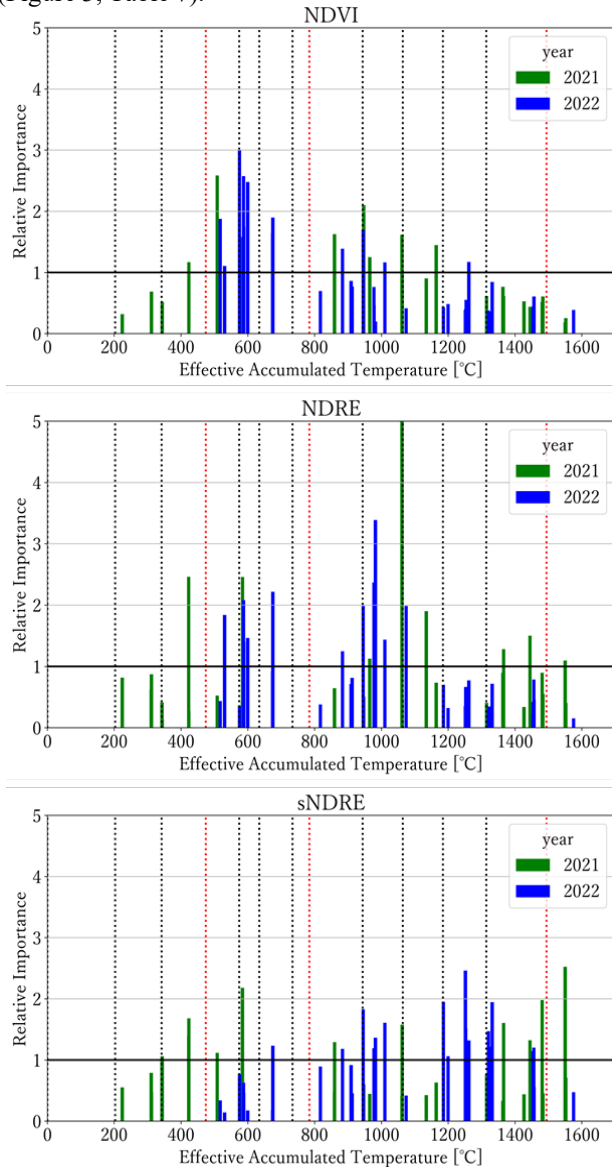


Figure 6: Relative Importance

For vegetation growth changes before and after fertilization, there were no monitoring data before fertilization included in the optimized period for either field (Table 6, Table 9).

Usually, additional fertilization is conducted on a day when EAT is around 500°C to 650°C (about 2 to 4 weeks before heading). Although sNDRE was not included in this period, NDVI and

NDRE were. However, at Yuguchi-8, all monitoring occurred after heading, and at Yuguchi, the first time was before young panicle formation and the second time during heading. In short, no monitoring was conducted between the start date of the optimized period and the fertilization date at either site. From the results of the optimized TSC period, it was not possible to visualize the growth before fertilization. Thus, vegetation differences are discussed using the results for the entire period (Table 6). From the time-series trends of each cluster, it can be seen that NDVI and NDRE increased between the first and second monitoring days. This suggests that nutrient supplementation with fertilizers improves vegetation and stress conditions. In addition, sNDRE is not suitable for comparing these conditions with other days because of the standardization of each day.

As described above, TSC of the VIs was able to visualize the health status of paddy rice and predict the appropriate fertilizer amount. On the other hand, in order to further improve predictive.

Table 9: Optimized period of EAT of each VI

VI	Optimized period of EAT [°C]	Date for a Normal Year
NDVI	509 – 913	Jul. 10 – Aug. 10
NDRE	588 – 1063	Jul. 16 – Aug. 21
sNDRE	860 – 1332	Aug. 6 – Sep. 11

Table 10: Results of mesh classification match percentage between RF and TSC and McNemar's test

VI	Site	p_{ent}	p_{opt}	p-value
NDVI	Yuguchi-8	96.3%	100.0%	< 0.001
	Yuguchi	96.5%	99.4%	0.002
NDRE	Yuguchi-8	94.3%	99.0%	< 0.001
	Yuguchi	96.0%	98.1%	0.050
sNDRE	Yuguchi-8	91.0%	95.9%	0.003
	Yuguchi	93.4%	99.4%	< 0.001

first is the use of a broader range of wavelengths beyond visible light. Some of the VIs that have been developed so far use these bands (e.g., NDNI, CAI, etc.) [5], [25]. By using these VIs after confirming their effectiveness with ground truth data such as RGB images and site inspections, it becomes possible to visualize water stress, nutritional deficiencies, pest infestation, and so on. For ensuring the accuracy and reliability, it is necessary to verify them using detailed measurement data obtained from sensors such as air temperature and water temperature in mesh unit. Future research should utilize such ground truth data for TSC to observe various aspects of crop conditions. The second is to perform accurate spatial analysis. In this paper, for fast processing, the data used in the TSC was reduced in size by determining the mesh size (apprxi

mately 3m x 3m) based on the resolution. It is desirable to perform TSC with various mesh sizes and verify the mesh size that increases the accuracy of the optimal fertilizer amount prediction and yield prediction. Also, the spatial variability of vegetation indices within the rice field and its implications for fertilizer management may be caused by the evenness of the rice field, location of water outlets and water flow within the rice field, and so forth. We hope to identify the causes of this spatial heterogeneity using spatial analysis techniques and the analytical methods of this study.

4.2. Evaluation of Optimization

In the previous section 4.1, it was analyzed in both fields that the appropriate fertilizer amount was the lowest amount field by the TSC using the optimized period. The bottom panel of Table 5 shows the evaluation of this analysis from the viewpoint of yield. As mentioned in the previous chapter, this is the p-value of the test for significant differences in yield between fields when the null hypothesis is set as "the average of sampled yields of all rice fields are equal." Based on this test, the null hypothesis was adopted, even at the 10% significance level. In other words, it cannot be said that there is a difference in yield between paddy fields, and it also cannot be said that changing the fertilizer amount will change the yield. Therefore, the field with the least amount of fertilizer is appropriate from the viewpoint of avoiding fertilizer costs, excessive fertilization, and environmental impacts. This result agrees with the TSC analysis results.

In local practice, the fertilizer applied to all fields is 4.2 gN/m². Assuming that this was changed to an appropriate 2.8 gN/m², the fertilizer was reduced to 87 and 91 kg, and the amount of leached nitrogen was reduced to 0.070mg/L for both Yuguchi-8 and Yuguchi. It was small compared to the water pollution standards. This is the case when fertilizer is applied during irrigation, and the leaching amount is only approximately 3% of that during surface drainage [26], [27][28]. Therefore, TSC method reduces the amount of excess fertilizer used, so it is expected to reduce the environmental impact. Furthermore, the development of such appropriate fertilization techniques will contribute to the sustainability of agriculture by creating soil that can produce food over the long-term without degrading the environment [29]. And continued analysis of this study will promote long-term soil health by reducing chemical fertilizers and increasing organic ones without reducing yields. This is a topic for future work.

As described above, the amount of excess fertilizer was estimated by using TSC for VI from UAV. In order to ensure accuracy and reliability, this research will need to address the following three things in the future. First is the use of data fusion technology. This is important to enhance the predictive power of the model and provide a more comprehensive understanding of factors influencing crop response to fertilization. Future research would like to try to analyze differences in soil and past crop management practices for each rice field.

5. Conclusions

In this research, the VIs time-series data were obtained using a UAV. Additionally, the monitoring dates were converted into growth stages (EAT) using a paddy rice growth model from related research [19], [20]. On this data, three analyzes were performed. In the first analysis, it was possible to visualize healthy vegetation growth and stress in paddy rice

using the TSC. We also confirmed that healthy vegetation growth and stress of crops were improved by fertilizer. In the second analysis, the Kruskal–Wallis test confirmed the appropriate amount from the results of TSC. In the third analysis, the optimized period was determined based on the importance of each independent variable using RF. Based on these findings, our work have discovered the technologies can help reduce fertilizer costs, excessive fertilization and environmental impacts, and promote the use of UAV.

A future challenge is the development of a growth-prediction model. This study deals with ex-post evaluations, such as the visualization and classification of crop conditions. Also it is necessary to make future predictions for crop yields, early disease detection, and variable fertilization using VIs. Currently, there are no absolute standards for VIs, and no study has been found that generalizes the desirable values at each growth stage. However, a research has established a target NDVI for each growth stage using a portable device for NDVI measurement [30], [31]. This study collects and analyzes VI data via UAVs to improve productivity and reduce costs. For this purpose, we will develop a system that uses deep learning to provide decision support for fertilization in natural language based on the features of monitoring images [32] and methods such as farm income prediction based on yield prediction using regression, and so on. Then, it would be desirable to be able to connect UAVs with these systems and provide information to farmers in real time. As the IoT advances, security issues are a concern, so it will be important to develop autonomous decentralized systems that increase data tamper resistance using blockchain technology [33], [34], [35], [36].

Conflict of Interest

The authors declare no conflict of interest.

Acknowledgment

The authors would like to thank the Research Center for Industrial Science and Technology, Iwate University, and the farmers in the experimental field for providing monitoring and yield survey data. We would also like to thank Editage (www.editage.jp) for English language editing. Finally, we are grateful to the referees for their helpful comments.

References

- [1]. T. Ito, K. Minamino and S. Umeki, "Analysis of Vegetation Indices by Time Series Clustering of Drone Rice Monitoring Data," 3rd International Symposium on Electrical, Electronics and Information Engineering (ISEEIE 2023), 2023, DOI: 10.1049/icp.2023.1853.
- [2]. Ministry of Agriculture, Forestry and Fisheries, "2020 nen nou-rin-gyou census kekka no gaiyou (kakuteichi)," URL: https://www.maff.go.jp/j/tokei/kekka_gaiyou/noucen/2020/index.html, [Accessed 5 February 2024], (article in Japanese).
- [3]. K. Miyama, "Nou-sakumotsu · dozyou no bunkou-hansya-tokusei - nou-you-chi he no remote sensing gizyutsu no tekiyou-sei (I)," Journal of the Agricultural Engineering Society, Japan, **56**(12):1197-1202, 1988, (article in Japanese).
- [4]. J. L. Hatfield and J. H. Prueger, "Value of Using Different Vegetative Indices to Quantify Agricultural Crop Characteristics at Different Growth Stages under Varying Management Practices," Remote Sensing, **2**(2):562-578, 2010, DOI: 10.3390/rs2020562.
- [5]. J. Xue and B. Su, "Significant Remote Sensing Vegetation Indices: A Review of Developments and Applications," Journal of Sensors, **2017**:1-17, 2017, DOI: 10.1155/2017/1353691

- [6]. K. Tanaka and A. Kondoh, "Mapping of Rice Growth Using Low Altitude Remote Sensing by Multicopter," *Journal of The Remote Sensing Society of Japan*, **36**(4):373-387, 2016, DOI: 10.11440/rssj.39.S1.
- [7]. K. Harashina, K. Yamamoto, M. Maki, Y. Muto and E. Kurashima, "Monitoring Growth of Water-seeded Rice in Tsunami-stricken Paddy Fields Using UAV-mounted Multispectral Sensor," *Journal of the Japanese Society of Irrigation, Drainage and Rural Engineering*, **87**(2):121-126, 2019, (article in Japanese with a title in English).
- [8]. A. Matsuzaki, Inasaku dai hyakka dai 2 han dai 3 kan saibai no zissai/sehigizyutsu, Rural Culture Association, 2004, (article in Japanese).
- [9]. Kubota Co., Ltd., "Mizu to hiryuu ni yoru control | tanbo no kanri to higaitaisaku | okome ga dekirumade | Kubota no tanbo [manande tanoshii! tanbo no sougou zyouhou site]," URL: <https://www.kubota.co.jp/kubotatanbo/rice/management/manure.html>, [Accessed 21 December 2023], (article in Japanese).
- [10]. National Institute of Science and Technology Policy, "NISTEP PDF cover 200612," URL: <https://nistep.repo.nii.ac.jp/record/5536/files/NISTEP-STT069.pdf>, [Accessed 21 December 2023], (article in Japanese).
- [11]. Ministry of the Environment, "Suishitsu-osen ni kakawaru kankyo-kizyun," URL: <https://www.env.go.jp/kijun/mizu.html>, [Accessed 7 February 2024], (article in Japanese).
- [12]. T. Ito, K. Minamino and S. Umeki, "Analysis of Vegetation Indexes by Time Series Clustering of Drone Rice Monitoring Data," *The 21st Forum on Information Technology (FIT2022)*, **21**(4):105-110, 2022, (article in Japanese with a title in English).
- [13]. T. Ito, K. Minamino and S. Umeki, "Analysis of Fertilization Effects on Rice and Wheat by Time-Series Clustering of Vegetation Index Data," *Proceedings of the 5th International Symposium on Advanced Technologies and Applications in the Internet of Things (ATAIT 2023)*, 2023.
- [14]. Da-Jiang Innovations Science and Technology Co., Ltd., "AGRAS MG-1S Series - DJI," URL: <https://www.dji.com/mg-1s>, [Accessed 8 February 2024].
- [15]. Da-Jiang Innovations Science and Technology Co., Ltd., "P4 MultispectralDJI," URL: <https://www.dji.com/p4-multispectral>, [Accessed 8 February 2024].
- [16]. A. Karnieli, N. Agam, R. T. Pinker, M. Anderson, M. L. Imhoff, G. G. Gutman, N. Panov and A. Goldberg, "Use of NDVI and Land Surface Temperature for Drought Assessment: Merits and Limitations," *Journal of Climate*, **23**(3):618-633, 2010, DOI: 10.1175/2009JCLI2900.1
- [17]. H. Zheng, W. Ji, W. Wang, J. Lu, D. Li, C. Guo, X. Yao, Y. Tian, W. Cao, Y. Zhu and T. Cheng, "Transferability of Models for Predicting Rice Grain Yield from Unmanned Aerial Vehicle (UAV) Multispectral Imagery across Years, Cultivars and Sensors," *Drones*, **6**(12:423):1-19, 2022, DOI: 10.3390/drones6120423.
- [18]. [18] L. Osborn, "NDVI vs. NDRE: What's the Difference? - Sentra," URL: <https://sentra.com/resources/articles/ndvi-vs-ndre-whats-the-difference/>, [Accessed 8 February 2024].
- [19]. E. Kanda, Y. Torigoe and T. Kobayashi, "A Model to Estimate the Increase of Leaf Number on the Main Culm of the Rice Plant," *Japanese Journal of Crop Science*, **69**(4):540-546, 2000, DOI: 10.1626/jcs.69.540, (article in Japanese with an abstract in English).
- [20]. E. Kanda, Y. Torigoe and T. Kobayashi, "A Simple Model to Predict the Developmental Stages of Rice Panicles Using the Effective Accumulative Temperature," *Japanese Journal of Crop Science*, **71**(3):394-402, 2002, DOI: 10.1626/jcs.71.394, (article in Japanese with an abstract in English).
- [21]. A. K. Jain, M. N. Murty and P. J. Flynn, "Data Clustering: A Review," *ACM Computing Surveys*, **31**(3):264-323, 1999, DOI:10.1145/331499.331504.
- [22]. R. Tavenard, "tslearn.clustering.TimeSeriesKMeans — tslearn 0.6.3 documentation," URL: https://tslearn.readthedocs.io/en/stable/gen_modules/clustering/tslearn.clustering.TimeSeriesKMeans.html, discriminant method of elbow point for the optimal number of clusters in clustering algorithm," *EURASIP Journal on Wireless Communications and Networking*, **31**:1-16, 2021, DOI: 10.1186/s13638-021-01910-w.
- [24]. S. Ronaghan, "The Mathematics of Decision Trees, Random Forest and Feature Importance in Scikit-learn and Spark," URL: <https://towardsdatascience.com/the-mathematics-of-decision-trees-random-forest-and-feature-importance-in-scikit-learn-and-spark-f2861df67e3>, [Accessed 11 February 2024].
- [25]. The IDB Project, "Index DataBase," URL: <https://www.indexdatabase.de/>, [Accessed 23 April 2024].
- [26]. Toyama Prefecture, "Chika-sui kanyou no suishin ni mukete," URL: <https://www.pref.toyama.jp/documents/7739/00745883.pdf>, [Accessed 17 February 2024], (article in Japanese).
- [27]. C. Imagawa, "Nitrogen Dynamics Modeling to Support Land and Water Management in Rice Paddy Watershed," *Soil/Water Research Group Materials*, **30**, 2013, (article in Japanese with a title in English).
- [28]. M. Tsuji and M. Takei, "Degrees of Water Purification in Cultivated Rice Fields and Fallow Fields," *Research bulletin of the Aichi-ken Agricultural Research Center*, **43**:1-6, 2011, (article in Japanese with an abstract in English).
- [29]. M. M. Tahat, K. M. Alananbeh, Y. A. Othman and D. I. Leskova, "Soil Health and Sustainable Agriculture," *Sustainability*, **12**(12), 2020, DOI: 10.3390/su12124859.
- [30]. NIKON-TRIMBLE CO., LTD., "GreenSeeker 2," URL: https://www.nikon-trimble.co.jp/products/product_detail.html?tid=428, [Accessed 15 February 2024].
- [31]. Y. Kaneta, M. Nishida, F. Takakai and T. Sato, "New growth diagnosis standards of high-yielding rice and demonstration of high yielding using NDVI by GreenSeeker handheld crop sensor," *Japanese Journal of Soil Science and Plant Nutrition*, **91**(6):417-425, 2020, DOI: 10.20710/dojo.91.6_417, (article in Japanese with an abstract in English).
- [32]. S. Ayoub, Y. Gulzar, F. A. Reegu and S. Turaev, "Generating Image Captions Using Bahdanau Attention Mechanism and Transfer Learning," *Symmetry*, **14**(12), 2022, DOI: 10.3390/sym14122681.
- [33]. F. A. Reegu, H. Abas, Y. Gulzar, Q. Xin, A. A. Alwan, A. Jabbari, R. G. Sonkamle and R. A. Dziyauddin, "Blockchain-Based Framework for Interoperable Electronic Health Records for an Improved Healthcare System," *Sustainability*, **15**(8), 2023, DOI: 10.3390/su15086337.
- [34]. A. A. Dar, M. Z. Alam, A. Ahmad, F. A. Reegu and S. A. Rahin, "Blockchain Framework for Secure COVID-19 Pandemic Data Handling and Protection," *Computational Intelligence and Neuroscience*, **2022**(7025485):1-11, 2022, DOI: 10.1155/2022/7025485.
- [35]. M. Z. Alam, F. Reegu, A. A. Dar and W. A. Bhat, "Recent Privacy and Security Issues in Internet of Things Network Layer: A Systematic Review," *2022 International Conference on Sustainable Computing and Data Communication Systems (ICSCDS)*, 2022, DOI: 10.1109/ICSCDS53736.2022.9760927.
- [36]. F. A. Reegu, W. A. Bhat, A. Ahmad and M. Z. Alam, "A review of importance of blockchain in IOT security," *International Conference on Emerging Trends in Materials, Computing and Communication Technologies (ICETMCCT 2021)*, **2587**(1), 2023, DOI: 10.1063/5.0150432.

Copyright: This article is an open access article distributed under the terms and conditions of the Creative Commons Attribution (CC BY-SA) license (<https://creativecommons.org/licenses/by-sa/4.0/>).